Available online at www.sciencedirect.com
ScienceDirect
Progress in Natural Science 19 (2009) 1281–1286
Progress in Natural Science
www.elsevier.com/locate/pnsc

Compressibility of a natural kyanite to 17.5 GPa

Xi Liu [a,b,*], Sean R. Shieh [c], Michael E. Fleet [c], Lifei Zhang [a,b]

[a] Key Laboratory of Orogenic Belts and Crustal Evolution, MOE, Peking University, Beijing 100871, China
[b] School of Earth and Space Sciences, Peking University, Beijing 100871, China
[c] Department of Earth Sciences, University of Western Ontario, London, Ont., Canada N6A 5B7

Received 19 November 2008; received in revised form 23 March 2009; accepted 8 April 2009

Abstract

The compressional behaviour of a natural kyanite, $(Al_{1.99}Fe_{0.01})SiO_5$, has been investigated to about 17.5 GPa at 300 K using a diamond-anvil cell and synchrotron X-ray diffraction. The pressure–volume data fitted to the third-order Birch–Murnaghan equation of state (EoS) yield an isothermal bulk modulus (K_{0T}) of 192 ± 6 GPa and pressure derivative (K'_{0T}) of 6 ± 1. When K'_{0T} is fixed as 4, the derived K_{0T} is 201 ± 2 GPa. These values are in excellent agreement with most experimental determinations in the literature. Consequently, it can be concluded that the compressibility of kyanite under high pressures has been accurately constrained.

Keywords: Compressibility; High-pressure; Isothermal bulk modulus; Kyanite; Synchrotron X-ray diffraction

1. Introduction

Kyanite, the high-pressure polymorph of Al_2SiO_5 [1], is an important constituent phase for the materials of continental crust and pelagic sediment at pressures from ~1 to ~16 GPa [2,3]. It plays a significant role in a large number of geological reactions, which may involve phases like paragonite, zoisite, lawsonite, pumpellyite, chloritoid, staurolite, and stishovite [4–8]. In order to fully understand these reactions and their phase relations, apparently, it is necessary to accurately constrain the thermodynamic properties of kyanite, one of which is the elasticity.

The elastic properties of kyanite have not been well determined so far, although quite a few studies with different methods including high pressure experimentation and theoretical calculation have been carried out [9–16]. Brace et al. [9] conducted a pioneering but preliminary experimental investigation on a synthetic mixture of kyanite powder and powder of lead or copper and determined a bulk modulus (K_{0T}) of 130 ± 10 GPa for kyanite. With an experimental study of the decomposition of kyanite to stishovite and corundum, Irifune et al. [10] thermodynamically arrived at the conclusion that the bulk modulus of kyanite is probably around 202 ± 15 GPa (K'_{0T} of all involved phases fixed as 4). Both Comodi et al. [12] and Yang et al. [13] conducted a single-crystal X-ray diffraction study on kyanite, and they constrained the bulk modulus of kyanite to be 160 ± 3 and 193 ± 1 GPa (K'_{0T} fixed as 4), respectively. The most recent experimental investigation on the elasticity of kyanite was done by Friedrich et al. [16], who obtained the bulk modulus of kyanite to be 190 ± 3 (K'_{0T} fixed as 4). On the other hand, theoretical calculations conducted to investigate the compressibility of kyanite also show some discrepancies [11,14,15]. Molecular dynamics simulation determined a value of 197 GPa for the isothermal bulk modulus of kyanite [11], whereas *ab initio* simulation suggested a value of 172 GPa (K'_{0T} fixed as 4.1) [14]. Using density functional theory with a generalized

* Corresponding author. Tel.: +86 10 6275 3585; fax: +86 10 6275 2996.
E-mail address: xi.liu@pku.edu.cn (X. Liu).

1002-0071/$ - see front matter © 2009 National Natural Science Foundation of China and Chinese Academy of Sciences. Published by Elsevier Limited and Science in China Press. All rights reserved.
doi:10.1016/j.pnsc.2009.04.001

gradient approximation, Winkler et al. [15] reported a value of 178 GPa.

This study was designed to evaluate the compressional behaviour of kyanite at high pressure using a diamond-anvil cell and synchrotron X-ray diffraction.

2. Experimental details

Bluish crystals of a natural kyanite with an unknown source were carefully crushed and thoroughly ground under acetone in an agate mortar. Part of the powder product was analysed by an X-ray fluorescence spectrometer hosted at the Department of Earth Sciences, University of Western Ontario; the analysis showed that this natural kyanite has a composition of 36.62% SiO_2, 62.72% Al_2O_3 and 0.31% Fe_2O_3 (by weight), with all other components negligible. No specific method was used to check the charge state of iron; according to Burns [17], rather, we assumed all iron as Fe^{3+}. Consequently, the chemical formula of our natural kyanite is approximately $(Al_{1.99}Fe_{0.01})SiO_5$.

Part of the powder product was checked by a powder X-ray diffractometer hosted at the School of Earth and Space Sciences, Peking University (X'Pert Pro MPD system; Cu Kα1 X-ray radiation). Kyanite was confirmed to be the only solid crystalline phase, with the unit-cell parameters $a = 7.115(2)$ Å, $b = 7.841(2)$ Å, $c = 5.573(2)$ Å, $\alpha = 90.01°(3)$, $\beta = 101.13°(3)$ and $\gamma = 105.96°(3)$, which are essentially identical to those values given by the JCPDS reference pattern card 11-46. Its ambient pressure unit-cell volume was determined to be 292.8 ± 0.1 Å^3, slightly smaller than that of the kyanite from Minas Gerais, Brazil (293.9 ± 0.3 Å^3 in [12]; 293.31 ± 0.02 Å^3 in [13]). This minor volume difference might be caused by the difference in the compositions of these two kinds of kyanite; the chemical formula of the kyanite from Minas Gerais, Brazil, is $Al_{1.98}Fe_{0.02}SiO_5$ (iron was assumed to present as Fe^{3+}) [12].

We conducted our high-pressure angle dispersive X-ray diffraction experiments up to about 17.5 GPa with a symmetrical diamond-anvil cell at the beamline X17C, National Synchrotron Light Source, Brookhaven National Laboratory, USA. In general, the experimental techniques used here were very similar to those reported by Liu et al. [18]. T301 stainless steel plates with an initial thickness of 250 μm were used as gaskets. The central area of the plates was pre-indented to a thickness of about 30 μm, and a hole of 150 μm in diameter was subsequently eroded electrically. The kyanite powder, along with a couple of tiny ruby balls, was loaded with the pressure medium (a 4:1 methanol–ethanol mixture which should solidify at about 10 GPa at 300 K) into the hole in the gasket. With the ruby fluorescence method [19], the experimental pressure was measured before and after each X-ray analysis. The incident synchrotron radiation beam was monochromatized to a wavelength of 0.4066 Å, and its beam size was collimated to a diameter of $\sim 25 \times 20$ μm^2. The X-ray diffraction pattern of the sample at certain pressure was collected with an exposure time of 10 min using an online CCD detector, and later integrated as a function of 2θ to give the conventional one-dimension X-ray profile using the Fit2D program [20].

Kyanite has the lowest symmetry ($P\bar{1}$) and large unit-cell parameters [12,13]. Consequently, it has to be probed, as required by the Bragg Law, by X-ray radiation with long wavelength, in order to achieve good resolution. As shown in Fig. 1, even with the Cu Kα1 X-ray radiation, some peak overlapping is still inevitable; for instance, peak 2 −1 1 slightly overlaps with peak −2 −1 1, peak −1 1 2 with peak −1 3 0, peak 0 1 2 with peak 0 3 0, peak −2 1 2 with peak −2 3 0, peak 1 1 2 with peak −2 −1 2, peak 1 3 1 with peak −3 3 1. Only with great care could these overlapping peaks be successfully separated by the Peakfit program. The shorter wavelength of the synchrotron X-ray radiation exacerbates the problem, and more intense peak overlapping has been observed (Fig. 1). Lucky enough, however, there are still many free-standing peaks as shown in Fig. 1, and not all of the overlapping peaks are completely unresolvable by the Peakfit program. Therefore, the unit-cell parameters of kyanite, calculated by refining the unit cell using the positions of the strongest and most unambiguous diffraction peaks, such as −1 1 1, 0 2 0, 2 0 0, −2 1 1, 0 2 1, −2 2 0, 0 4 0, −4 1 1, and 1 1 3, can be constrained with high confidence. The good agreement in the unit-cell parameters of kyanite constrained by the conventional powder X-ray radiation and by the synchrotron is an indicator of the success of the experimental method used in this study.

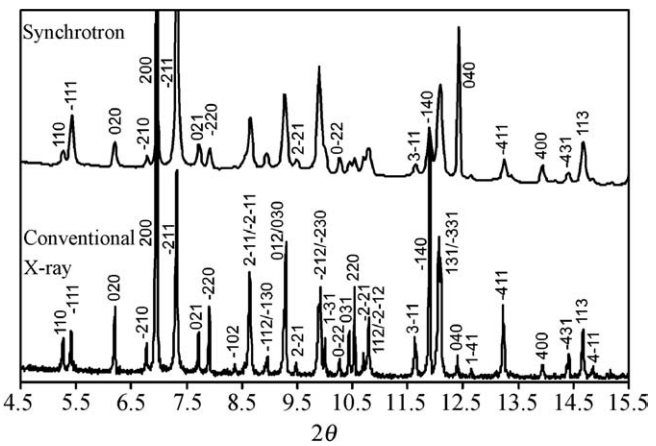

Fig. 1. Ambient synchrotron powder X-ray diffraction (wavelength = 0.4066 Å) versus conventional powder X-ray diffraction (Cu Kα1; a wavelength of 1.5405 Å was used in collecting the data which, when plotted here, have been recalculated to the wavelength of 0.4066 Å, for the purpose of comparison). Apparently, the synchrotron analysis has a lower resolution, due to the shorter wavelength of the synchrotron X-ray radiation and the low symmetry ($P\bar{1}$) of kyanite. In order to show the data clearly, overlapping but probably resolvable major peaks and minor peaks from the kyanite sample are not indexed for the synchrotron powder X-ray diffraction pattern.

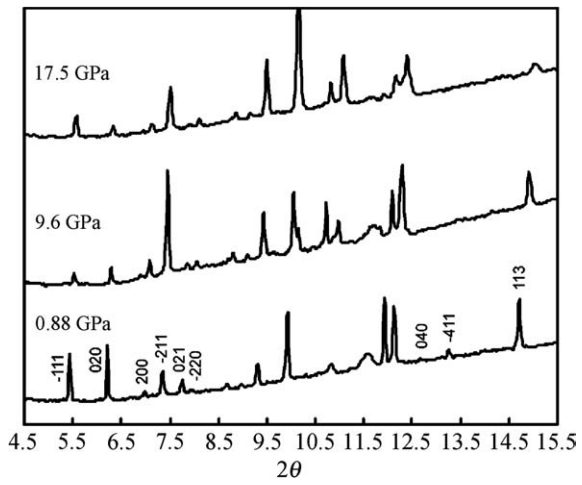

Fig. 2. Examples of the X-ray diffraction patterns of kyanite at 0.88, 9.6 and 17.5 GPa. Overlapping but probably resolvable major peaks and minor peaks from the kyanite sample and peaks from the gasket of stainless steel are not indexed for the purpose of clarity.

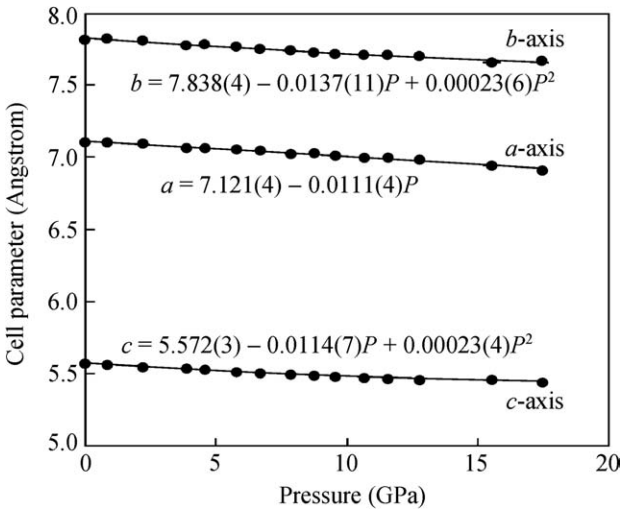

Fig. 3. Pressure dependence of the unit-cell parameters a, b and c of kyanite at 300 K. Note that for most data points their error bars are approximate to or smaller than the symbols.

3. Result and discussion

Experiments were carried out up to 17.5 GPa at room temperature. No phase transition, transformation or amorphization was found over this pressure range (Fig. 2), which in general confirmed the observation made by Friedrich et al. [16]. According to the experimental and theoretical investigations in the literature [7,8,10,14,21–23], kyanite, at room temperature, can be stable at pressures up to only about 12 GPa. Apparently, the data we collected at pressures higher than 12 GPa were from the metastable field of kyanite.

The effect of pressure on the unit-cell parameters is summarized in Table 1 and graphically shown in Figs. 3 and 4. The pressure dependence of the unit-cell parameter a can be represented by the regression equation $a = 7.121(\pm 4) - 0.0111(\pm 4)P$, that of the unit-cell parameter b by $b = 7.838(\pm 4) - 0.0137(\pm 11)P + 0.00023(\pm 6)P^2$, and that of the unit-cell parameter c by $c = 5.572(\pm 3) - 0.0114(\pm 7)P + 0.00023(\pm 4)P^2$, with a, b, c in Å and P in GPa (Fig. 3). This observation is not completely consistent with the observations made by Yang et al. [13] and Comodi et al. [12], in which unit-cell parameters a, b, c of kyanite varied linearly with pressure; Yang et al. [13] and Comodi et al. [12] limited the pressure of their experiments up to 4.56 and 5.80 GPa, respectively, so that the effect of pressure on these unit-cell parameters might have not fully shown up. The variation of the unit-cell parameters α, β and γ of kyanite with pressure is shown in Fig. 4: α seems to increase while β and γ seem to decrease slightly with pressure increase. This observation is generally in agreement with Yang et al. [13], although our synchrotron data on a powdered sample are not as accurate as the

Table 1
Unit-cell parameters of kyanite at different pressures.

P (GPa)	a (Å)	b (Å)	c (Å)	α (°)	β (°)	γ (°)	V (Å^3)
0.0001	7.114(1)	7.835(2)	5.568(1)	89.94(2)	101.20(2)	105.91(2)	292.33(9)
0.88(0)	7.104(3)	7.828(4)	5.560(3)	89.92(7)	101.22(8)	106.16(9)	290.84(19)
2.21(3)	7.097(1)	7.814(2)	5.548(1)	89.88(4)	101.10(3)	106.41(4)	289.15(9)
3.87(8)	7.071(1)	7.777(3)	5.536(1)	89.87(3)	101.26(1)	106.12(2)	286.4(1)
4.58(6)	7.072(4)	7.784(3)	5.528(3)	90.03(7)	101.13(5)	106.24(6)	286.2(2)
5.8(2)	7.060(3)	7.768(2)	5.517(2)	90.01(5)	101.09(4)	106.36(5)	284.4(1)
6.70(8)	7.052(2)	7.756(2)	5.506(1)	89.97(4)	101.10(3)	106.36(4)	283.1(1)
7.9(2)	7.028(2)	7.746(2)	5.500(1)	90.01(4)	101.14(3)	106.33(4)	281.5(1)
8.8(1)	7.032(5)	7.732(5)	5.493(3)	90.02(9)	101.03(7)	106.41(9)	280.7(2)
9.6(1)	7.020(2)	7.725(1)	5.481(1)	90.03(3)	101.10(3)	106.33(3)	279.41(6)
10.7(2)	7.003(4)	7.714(3)	5.471(2)	90.14(7)	100.99(6)	106.26(7)	278.0(2)
11.6(2)	7.000(2)	7.716(1)	5.468(1)	90.20(4)	101.03(4)	106.22(4)	277.85(8)
12.8(2)	6.986(2)	7.705(2)	5.459(1)	90.22(4)	100.95(4)	106.26(4)	276.48(9)
15.5(3)	6.944(3)	7.667(4)	5.458(3)	89.85(1)	101.38(7)	106.11(7)	273.2(2)
17.5(1)	6.910(3)	7.673(3)	5.445(2)	90.13(6)	101.08(4)	106.34(4)	271.4(1)

Note: X-ray data at ambient pressure were collected on a kyanite powder sample loosely packed into a small hole (400 μm across) in a stainless steel plate; the numbers in parentheses represent one standard deviation in the right-most digit.

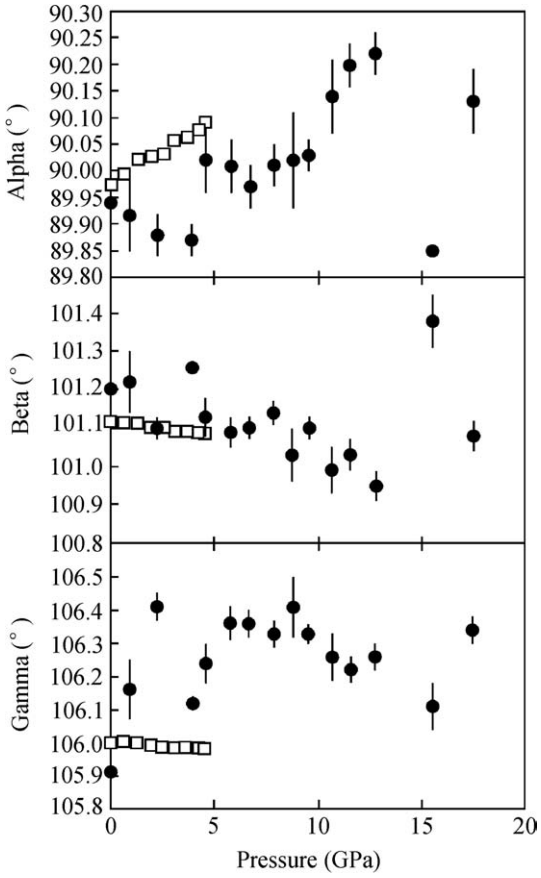

Fig. 4. Pressure dependence of the unit-cell parameters α, β and γ of kyanite at 300 K. Circles stand for the data collected in this investigation, whereas squares stand for the data in Yang et al. [13]. The two off-trend data at 15.5 and 17.5 GPa might reflect the cumulated strain caused by the solidification of the pressure medium.

single-crystal X-ray data of Yang et al. [13]. One interesting phenomenon shown by our data in Fig. 4 is that the unit-cell parameter γ seems to have a large jump when pressure is first applied to the sample (data at 0.0001 versus data at 0.88 GPa).

The P–V data of kyanite from this study are compared in Fig. 5 with the P–V data collected by Yang et al. [13] and Comodi et al. [12]. Although the zero-pressure volumes are slightly different, the compressibility of kyanite established in our study is much comparable to that determined by Yang et al. [13], since the trends shown by these two sets of data are almost parallel. The data from Comodi et al. [12], however, show a much more compressible property for kyanite.

In order to determine the elastic parameters, the P–V data from our study have been fitted to the third-order Birch–Murnaghan equation of state [24] by a least-squares method:

$$P = 3K_{0T}f_E(1+2f_E)^{\frac{5}{2}}\left[1+\frac{3}{2}(K'_{0T}-4)f_E\right] \quad (1)$$

where P is the pressure (GPa), K_{0T} the isothermal bulk modulus (GPa), K'_{0T} the first pressure derivative of K_{0T},

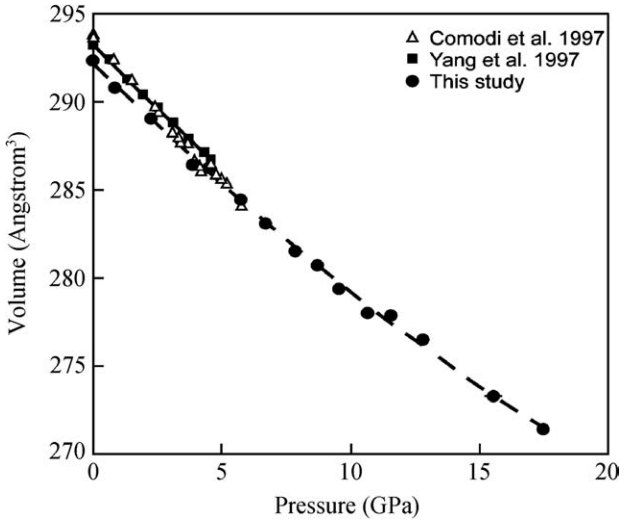

Fig. 5. Pressure–volume data of kyanite at 300 K observed in this study compared to those from Yang et al. [13] and Comodi et al. [12]. For clarity, only the data from Sample I and Sample IV in Comodi et al. [12] were plotted here. The solid curve represents the data from Yang et al. [13]; the dashed curve represents the third-order Birch–Murnaghan equation of state for kyanite obtained in this study. Note that for most data points their error bars are approximate to or smaller than the symbols.

and f_E the Eulerian definition of finite strain, which is $[(V_0/V)^{2/3}-1]/2$. In the Eulerian definition of finite strain, V_0 is the volume at zero pressure, whereas V is the volume at high pressure. When K'_{0T} is set as 4, the isothermal bulk modulus (K_{0T}) of kyanite is determined as 201 ± 2 GPa, whereas the zero-pressure volume is determined as 292.2 ± 0.1 Å^3. If K'_{0T} is not fixed, the results of our best data-fitting are $K_{0T} = 192 \pm 6$ GPa, $K'_{0T} = 6 \pm 1$ and $V_0 = 292.3 \pm 0.1$ Å^3.

The EoS data of kyanite can be evaluated by the plot of the normalized pressure (F; GPa) and the Eulerian strain (f_E), where F is defined as

$$F = \frac{P}{3f_E(1+2f_E)^{5/2}} \quad (2)$$

Fig. 6 shows that the datum points define an almost horizontal line, suggesting that a second-order equation of state or a third-order equation of state with K'_{0T} fixed as 4 can adequately describe the P–V data. We consequently conclude that the bulk modulus and its pressure derivative of kyanite determined in this investigation are about 201 GPa and 4, respectively.

The equations of state of kyanite constrained by the studies in the literature and this study are summarized in Table 2. With the exception of Comodi et al. [12], all other experimental investigations gave out similar values for the isothermal bulk modulus of kyanite (from 190 to 202 GPa with K'_{0T} fixed as 4), whatever the experimental methods (phase equilibrium study versus direct compression; Irifune et al. [10] versus Yang et al. [13], Friedrich et al. [16] and this study) and the experimental details (conventional single-crystal X-ray diffraction versus *in situ* powder

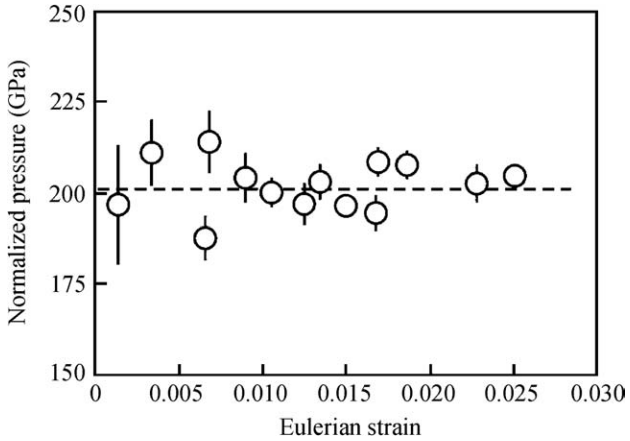

Fig. 6. Normalized pressure (F) as a function of Eulerian strain (f_E) for kyanite.

Table 2
Bulk modulus and first pressure derivative of kyanite.

Data source	K_{0T} (GPa)	K'_{0T}
Experimental study		
Irifune et al. [10]	202(15)[a]	4
Comodi et al. [12]	160(3)	4
Comodi et al. [12]	156(10)	5.6(5.5)
Yang et al. [13]	193(1)	4
Friedrich et al. [16]	190(3)	4
This study	201(2)	4
This study	192(6)	5.7(1.1)
Theoretical study		
Matsui [11]	197	
Oganov and Brodholt [14]	172	4.1
Winkler et al. [15]	178	

[a] The numbers in parentheses represent one standard deviation.

synchrotron X-ray diffraction; Yang et al. [13] versus Friedrich et al. [16] and this study) were. Comodi et al. [12] obtained a 20% smaller bulk modulus (160 GPa with K'_{0T} fixed as 4), which might have resulted from their poor choice of single crystals that were experimentally investigated. As they noticed, because of the perfect (1 0 0) cleavage of kyanite, all their selected crystals had [1 0 0] which coincided with the diamond-anvil cell axis, and therefore access to the reciprocal lattice was reduced in that direction. With all the experimental data under consideration, we summarily suggest that the bulk modulus and its pressure derivative of kyanite determined by the experimental studies are about 196 ± 6 GPa and 4, respectively. On the line of theoretical calculation, Matsui [11] gave out a value of 197 GPa, which perfectly matched with the experimental determination. Oganov and Brodholt [14] and Winkler et al. [15] suggested slightly smaller values of 172 and 178 GPa, respectively; this underestimation, however, might be due to the underbinding in the density functional theory with a generalized gradient approximation approach. Additionally, the values given by Oganov and Brodholt [14] and Winkler et al. [15] were for 0 K, instead of for room temperature.

Acknowledgements

We thank J. Hu for her help with the synchrotron X-ray diffraction experiment, H. Wang for his help with the conventional powder X-ray analysis and C. Wu for his help with the XRF analysis. We also thank an anonymous reviewer for the constructive comments which improved this paper. This investigation was financially supported by the Natural Sciences and Engineering Research Council of Canada and by the National Natural Science Foundation of China (Grant Nos. 40730314 and 40872033).

References

[1] Kerrick DM. The Al_2SiO_5 polymorphs. Reviews in mineralogy, vol. 22. Washington, DC: Mineralogical Society of America; 1990.
[2] Irifune T, Ringwood AE, Hibberson WO. Subduction of continental crust and terrigenous and pelagic sediments: an experimental study. Earth Planet Sci Lett 1994;126:351–68.
[3] Schmidt MW, Vielzeuf D, Auzanneau E. Melting and dissolution of subducting crust at high pressures: the key role of white mica. Earth Planet Sci Lett 2004;228:65–84.
[4] Chatterjee ND. The upper stability limit of the assemblage paragonite + quartz and its natural occurrences. Contrib Mineral Petrol 1972;34:288–303.
[5] Schreyer W. Experimental studies on metamorphism of crustal rocks under mantle pressures. Mineral Mag 1988;52:1–26.
[6] Poli S, Schmidt MW. H_2O transport and release in subduction zones: experimental constraints on basaltic and andesitic systems. J Geophys Res 1995;100:22299–314.
[7] Liu X, Nishiyama N, Sanehira T, et al. Decomposition of kyanite and solubility of Al_2O_3 in stishovite at high pressure and high temperature conditions. Phys Chem Miner 2006;33:711–21.
[8] Ono S, Nakajima Y, Funakoshi K. In situ observation of the decomposition of kyanite at high pressures and high temperatures. Am Mineral 2007;92:1624–9.
[9] Brace WF, Scholz CH, La Mori PN. Isothermal compressibility of kyanite, andalusite, and sillimanite from synthetic aggregates. J Geophys Res 1969;74:2089–98.
[10] Irifune T, Kuroda K, Minagawa T, et al. Experimental study of the decomposition of kyanite at high pressure and high temperature. In: The Earth's central part: its structure and dynamics. Tokyo: Terra Scientific Publishing; 1995. p. 35–44.
[11] Matsui M. Molecular dynamics study of the structures and moduli of crystals in the system $CaO–MgO–Al_2O_3–SiO_2$. Phys Chem Miner 1996;23:345–53.
[12] Comodi P, Zanazzi PF, Poli S, et al. High-pressure behavior of kyanite: compressibility and structural deformations. Am Mineral 1997;82:452–9.
[13] Yang H, Downs RT, Finger LW, et al. Compressibility and crystal structure of kyanite, Al_2SiO_5, at high pressure. Am Mineral 1997;82:467–74.
[14] Oganov AR, Brodholt JP. High-pressure phases in the Al_2SiO_5 system and the problem of aluminous phase in the Earth's lower mantle: *ab initio* calculations. Phys Chem Miner 2000;27:430–9.
[15] Winkler B, Hytha M, Warren MC, et al. Calculation of the elastic constants of the Al_2SiO_5 polymorphs andalusite, sillimanite and kyanite. Z Kristallogr 2001;216:67–70.
[16] Friedrich A, Kunz M, Winkler B, et al. High-pressure behavior of sillimanite and kyanite: compressibility, decomposition and indications of a new high-pressure phase. Z Kristallogr 2004;219:324–9.
[17] Burns RG. Mineralogical applications of crystal field theory. 2nd ed. Cambridge University Press; 1993.
[18] Liu X, Shieh SR, Fleet ME, et al. High-pressure study on lead fluorapatite. Am Mineral 2008;93:1581–4.

[19] Mao HK, Bell PM, Shaner JW, et al. Specific volume measurements of Cu, Mo, Pt, and Au and calibration of ruby R1 fluorescence pressure gauge for 0.006 to 1 Mbar. J Appl Phys 1978;49:3276–83.
[20] Hammersley J. Fit2D report. Grenoble, France: Europe Synchrotron Radiation Facility; 1996.
[21] Liu L. Disproportionation of kyanite to corundum plus stishovite at high pressure and high temperature. Earth Planet Sci Lett 1974;24:224–8.
[22] Schmidt MW, Poli S, Comodi P, et al. High-pressure behavior of kyanite: decomposition of kyanite into stishovite and corundum. Am Mineral 1997;82:460–6.
[23] Yong W, Dachs E, Withers AC, et al. Heat capacity and phase equilibria of hollandite polymorph of $KAlSi_3O_8$. Phys Chem Miner 2006;33:167–77.
[24] Birch F. Finite elastic strain of cubic crystals. Phys Rev 1947;71:809–924.